Anti-Silencing Function 1B Overexpression Affects Prognosis and Promotes Invasion in Cervical Carcinoma via Activation of Wnt/β-Catenin Signaling Pathway

Weijing Zhang
Sun yat-sen University Cancer Center
Han Li
Sun yat-sen University Cancer Center
Xiaoying Sun
Sun yat-sen University Cancer Center
Yongjie Shi
Guangzhou Medical University Second Affiliated Hospital
Yadi Yang
Sun yat-sen University Cancer Center
Chuanmiao Xie
Sun Yat-Sen University Cancer Center
Zhang Yanna (zhangyn@sysucc.org.cn)
Sun Yat-sen University Cancer Center https://orcid.org/0000-0002-1178-6059

Research Article

Keywords: ASF1B, Cervical carcinoma, Prognosis, Pelvic lymph node metastasis, Invasion, Wnt/β-catenin signaling

Posted Date: May 27th, 2021

DOI: https://doi.org/10.21203/rs.3.rs-345176/v1

Abstract

Background: Anti-silencing function 1B histone chaperone (ASF1B) has been identified to compensate for growth defects and sensitivity to replication stress. Recent studies demonstrated that ASF1B plays an important role in the tumorigenesis of human cancer. However, its relationship with clinical outcome of cervical carcinoma is unknown. Therefore, we aimed to investigate the expression pattern and clinical significance of ASF1B in cervical cancer and its role in regulating invasion and metastasis of cervical cancer cell lines.

Methods: Expression of ASF1B was analyzed in eight cervical cancer cell lines, and eight pairs of cervical cancer samples and the adjacent normal specimens, using real-time PCR and western blotting. Immunohistochemistry was used to analyze ASF1B expression in paraffin-embedded tissues from 147 cervical cancer patients. The association between ASF1B expression levels, clinicopathological parameters, and prognosis was analyzed statistically. Moreover, the biological function and potential mechanism of ASF1B in migration and invasion of cervical cancer cells were investigated by in vitro experiments and Western blotting.

Results: ASF1B mRNA and protein levels were overexpressed in cervical cancer cell lines and tissues compared with normal cells and adjacent normal cervical specimens. In paraffin-embedded cervical carcinoma tissues, upregulation of ASF1B protein was identified in 86 (58.5%) of 147 cases, and was remarkably associated with pelvic lymph node metastasis, lymphovascular space involvement, property of surgical margin, FIGO stage, sqaumous cell carcinoma antigen and poor survival. Cox analysis demonstrated that ASF1B expression was an independent risk predictor for survival in patients with cervical carcinoma. Additionally, down-regulation of ASF1B significantly inhibited invasion and migration of cervical cancer cells. Moreover, it was demonstrated that ASF1B regulated the Wnt/β-catenin pathway in cervical carcinoma.

Conclusions: This study suggested that ASF1B might serve as a important prognostic biomarker and therapeutic target for patients with cervical carcinoma.

Introduction

Cervical cancer is the third most common type of malignant gynecological tumor worldwide, ranking as the fourth main cause of cancer-associated deaths among women [1]. However, in view of the vast population base, it is reported that China accounts for 11.7 % (62,000 new cases) of the world's annual cervical cancer morbidity and 11.3 % (30,000 deaths) of annual cervical carcinoma mortality worldwide [2]. Despite current efforts and advances in early detection, treatment strategies, and research of cervical carcinoma, which have effectively lower the mortality rate of this malignancy, cervical carcinoma remains a prominent public health and economic burden in China. It is reported that patients with higher stage of International Federation of Gynecology and Obstetrics (FIGO), lymph node metastasis (LNM), lymphovascular space involvement or higher differentiation grade have poorer clinical outcomes [3]. In

the clinic, the squamous cell carcinoma antigen (SCC-Ag), an important serum biomarker of cervical carcinoma, has been used to determine LNM, prognosis, and recurrence in cervical cancer patients [4]. Moreover, a variety of novel oncogenes have been identified as significant biomarkers that are associated with unsatisfactory clinical outcome of cervical neoplasm [5–7]. However, they are not sufficiently powerful to predict clinical outcome, and their clinical applications are limited because of poor sensitivity and specificity. Hence, identifying new noninvasive, reliable, and effective biomarkers for the prognosis and treatment of cervical cancer, as well to improve our understanding of the mechanism of this disease, are urgently required.

ASF1B (anti-silencing function 1B histone chaperone), located on human chromosome 19 at 19p13.12, encodes a member of the H3/H4 family of histone chaperone proteins, which served an important role in histone dynamics during replication, transcription, and DNA repair [8]. Messiaen et al. indicated that ASF1B expression was specifically found in the germ cell lineage and ASF1B peak expression was significantly associated with meiosis [9]. Upregulation of ASF1B resulted in different transcriptional signatures consistent with enhanced cellular proliferation and decreased cellular apoptosis [10]. Previous studies indicated that ASF1B exerts important roles in the development of human cancer. Corpet et al. [11] showed that ASF1B is a prognostic predictor and proliferation indicator in early stage breast cancer. ASF1B expression is important for cellular proliferation, possibly during and after S phase, which is of great significance in progression of neoplasm. A recent study revealed that ASF1B, known as one of several chromatin regulators, is associated with local and metastatic relapse, and poor patient outcome in breast carcinoma [12].

In this study, we investigated the expression pattern of ASF1B in cancer of uterine cervix. The present study detected expression levels of ASF1B mRNA and protein in cervical cancer cell lines and surgical tissues of patients with cervical carcinoma. Correlations between ASF1B protein expression, and the clinicopathological risk factors and patient clinical outcomes were further analyzed. Furthermore, the function of ASF1B in uterine cervical cancer cell lines and its possible mechanism were investigated.

Materials And Methods

Cell lines and treatment

We purchased eight cell lines of cervical cancer (HeLa, C33A, SiHa, HeLa229, MS751, ME180, HCC94, and CasKi) from the Type Culture Collection of the Chinese Academy of Sciences (Shanghai, China), which were cultured in Roswell Park Memorial Institute RPMI-1640 medium (GIBCO, Gaithersburg, MD, USA). The medium was supplemented with 10% fetal bovine serum (FBS; Gibco; Thermo Fisher Scientific, Inc.) and 1% antibiotics penicillin-streptomycin. Cells were incubated at 37°C under a 5% CO_2-humidified atmosphere.

Samples and patient cohorts

The present study was carried out based on a cohort of 147 paraffin-embedded, surgical tissues of early-stage cervical carcinoma. All cases were clinically and histopathologically diagnosed with primary cervical carcinoma at the Sun Yat-sen University Cancer Center between 2006 to 2011. The FIGO (2009) standard was utilzed for peer-review of the clinical diagnoses and grading of the cases. World Health Organization (WHO) criteria was used for diagnoses of histological types and grades. For study purposes, the approval from the Medical Ethics Committee of the Sun Yat-sen University Cancer Center were obtained.

In this cohort, the 147 patients were diagnosed with IB1–IIA2 stage cervical carcinoma and all received a radical hysterectomy and lymphadenectomy. None of the patients had received preoperative radiotherapy, chemotherapy, or molecular-targeted therapy. Patients were followed up regularly in the clinic. We excluded patients who were lost of follow-up or loss of follow-up for short term. In the present study, according to the guidelines, sufferers with high-risk factors were arranged to receive radiotherapy and/or chemotherapy after surgical operations. The high-risk indicators comprise of PLNM, large tumor size (> 4 cm), deep stromal invasion, positive surgical margin, positive parametrial involvement, high differentiation grade, and positive lymphovascular space involvement. No patients received immunotherapy after surgical treatment.

Eight collected uterine cervical neoplasm samples and matched tumor-adjacent normal cervical tissues were frozen at − 80 °C and laid in liquid nitrogen prior to experiments. In addition, demographic and clinicopathological information for the 147 participants mentioned above were retrieved from impatient medical records and are summed up in Table 1. The median age of the cohorts was 46 years so that we used it as an age gap to divide the cases into two groups. In accordance to FIGO criteria, 61 patients were labeled as stage IB1; 24 as stage IB2; 42 as stage IIA1; and 20 as stage IIA2.

Table 1
Clinicopathological characteristics and tumor expression of ASF1B in patients with early-stage cervical cancer

Characteristic	Number of cases (%)
Age (years)	
≤ 46	79 (53.7)
> 46	68 (46.3)
FIGO stage	
Ib1	61 (41.5)
Ib2	24 (16.3)
IIa1	42 (28.6)
IIa2	20 (13.9)
Histological type	
Squamous carcinoma	138 (93.9)
Adenocarcinoma	9 (6.1)
Tumor size, cm	
< 4	107 (72.8)
≥ 4	40 (27.2)
Squamous cell carcinoma antigen, ng/ml	
≤ 1.5	67 (45.6)
> 1.5	80 (54.4)
Pelvic lymph node metastasis	
No	103 (70.1)
Yes	44 (29.9)
Tumor recurrence	
No	130 (88.4)
Yes	17 (11.6)
Vital status (at last follow-up)	
Alive	115 (78.2)
Dead	32 (21.8)

Characteristic	Number of cases (%)
Differentiation grade	
G1	53 (36.1)
G2	80 (54.4)
G3	14 (9.5)
Myometrium invasion	
< 1/2	52 (35.4)
≥ 1/2	95 (64.6)
Property of surgical margin	
No	137 (93.2)
Yes	10 (6.8)
Infiltration of parauterine organ	
No	140 (95.2)
Yes	7 (4.8)
Lymphovascular space involvement	
No	126 (85.7)
Yes	21 (14.3)
Chemotherapy	
No	65 (44.2)
Yes	82 (55.8)
Radiation therapy	
No	127 (86.4)
Yes	20 (13.6)
Expression of ASF1B protein	
Low or none	61 (41.5)
High	86 (58.5)

Real-time PCR analysis

The Total RNA from cell or tissue was extracted utilizing the Tri-Reagent (Sigma-Aldrich; Merck KGaA) on the basis of the manufacturer's protocol. The RNA quality was detected by An Agilent Bioanalyzer 2100. First-strand cDNA synthesis was carried out utilizing a Prime Script Reverse Transcriptase reagent Kit (Takara, Japan). Complementary DNA (cDNA) was amplified and quantified as follows. An initial amplification reaction utilizing specific primers of *ASF1B* was performed with a denaturation step at 95°C for 10 min, followed by 30 cycles at 95°C for 10 sec, primer annealing/extension at 60°C for 1 min. A final extension at 72°C for 5 min was carried out before the reaction was stopped and stored at 4°C. The PCR primers sequences of *ASF1B* are as follows: forward 5'-TGGACAGGAGTTCATCCGAGTG-3' and reverse 5'-GTCCCAGTTGATATGGAAGCGG-3'. The 2−ÄÄCt (cycle threshold) method were used, where the expression of *GADP*H was regarded as an endogenous standard to normalize the relative changes in *ASF1B* expression[5]. Primers for GADPH are as follows: forward 5'-AGAAGGCTGGGGCTCATTTGC-3' and reverse 5'-ACAGTCTTCTGGGTGGCAGTG-3'. All experiments were carried out in biological triplicate.

Western blotting analysis

Protein was extracted using RIPA buffer (BiYunTian, Shanghai, China) according to the manufacturer's protocol. Western blotting was carried out utilizing standard procedures according to our previous publication [3]. The protein samples (30 μg) were separated on 9% sodium dodecyl sulfate polyacrylamide gels and transferred onto polyvinylidene fluoride microporous membranes (Millipore, Billerica, MA, USA). After blocking with 5% non-fat milk for 2 h, the membranes were incubated with primary antibodies against ASF1B (No. 11011-1-AP, 1:1000; Proteintech, USA), cyclin D1 (No. ab134175, 1:2000, Abcam, USA), C-myc (No. ab32072, 1:1000, Abcam, USA), β-catenin antibody(No. #8480, 1:200; Cell Signaling, Danvers, MA, USA), α-Tubulin antibody(No. 11224-1-AP, 1:1000; Proteintech, USA), nuclear matrix protein P84 (No. Ab487, 1:1000, Abcam, USA) and GADPH (1:2,000; Sigma-Aldrich, St. Louis, MO, USA) overnight at 4 °C. Subsequently, the membranes were incubated with the corresponding secondary antibody (1:2000, anti-rabbit antibody or anti-mouse antibody, Abcam, Cambridge, UK) at room temperature for 1 h. Finally, ASF1B expression was explored utilizing enhanced chemiluminescence kit (Amersham Biosciences, Sweden).

Immunohistochemical staining and assessment

Immunohistochemistry (IHC) analysis was performed according to standard protocols, as previously mentioned [3] with anti-ASF1B antibodies (No. 11011-1-AP, Proteintech, USA). Paraffin-embedded specimens were prepared for IHC experiments from 147 patients with early-stage cervical carcinoma. Briefly, the 4-μm thickness paraffin-embedded sections were cut and baked at 60 °C for 30 min. The slides were then deparaffinized for 10 min in xylene (twice), and rehydrated through graduated alcohols to running distilled water to rinse. Submerging the sections into EDTA antigenic retrieval buffer and then microwaving were used for antigen retrieval. The tissue sections were blocked with 3 % hydrogen peroxide in methanol to quench the endogenous peroxidase activity, and then, the slides were incubated with 1 % bovine serum albumin for blocking nonspecific binding. The samples were rinsed with phosphate-buffered saline (PBS, PH 7.4). Next, the tissues were incubated with the primary antibodies against ASF1B (1:200) at 4 °C overnight. After washing, tissue sections were incubated with biotinylated

anti-rabbit secondary antibody (1:1000; Abcam) at room temperature, followed by incubation with streptavidin–horseradish peroxidase complex (Abcam). The samples were then submerged in 3,3-diaminobenzidine (DAB) and counterstained with 10% Mayer's hematoxylin, dehydrated, and mounted.

Each section was evaluated independently by two pathologists. Sections were viewed under a brightfield microscope. For ASF1B protein evaluation, the average staining intensity (SI) (0 = none; 1 = weak; 2 = modest and 3 = strong) of immunoreactive tumor cells were assessed. The percentage of positive stained tumor cells was given score as follows: 1 (1–25%); 2 (26–50%); 3 (51–75%), or 4 (> 75%). The staining index was calculated as the product of combining sensitivity and specificity. The log-rank test statistical analysis was applied to select the optimum cutoff score. Low expression of ASF1B protein was classified as 0 to 4 scores; high expression of ASF1B protein was classified as > 4 scores.

RNAi and transfection

For depletion of ASF1B, two sequences of ASF1B targeting siRNAs (Ribobio Inc Guangzhou, Guangdong, China) were as follows: siRNA#1: 5'-ACGAGUACCUCAACCCUGATT-3', siRNA#2: 5'-CGAGUGGGCUACUACGUCATT-3'. Transfection of siRNAs was carried out using Lipofectamine 2000 reagent (Invitrogen; Thermo Fisher Scientific, Inc.) following the protocols of the manufacturer.

Cell invasion assay

Migration of cells was assessed by cell invasion assay. Transwell insert chambers (Corning Incorporated, Corning, NY, USA) with 8-μm Matrigel-coated (BD Biosciences, USA) pore polycarbonate filters were used to test it. Cells plated in the absence or presence of siRNA at the density of 2×10^4 cells/well were incubated into the upper chamber with serum-free medium and allowed to invade in the lower chamber with 10% FBS medium as a chemotaxis agent. After 48h incubation, migratory cells on the lower surface of the membrane were stained with 0.5% crystal violet, examined by phase contrast microscopy(×200 magnification), photographed and counted. We performed all the experiments in triplicate independently.

Wound-healing assay

Cells(1×10^4 per well) were cultivated in a six-well plate separately. Untransfected cells and cells transfected wtih ASF1B siRNA were incubated in a quiescent medium overnight. Next, in confluent monolayers, a sterile 10-μl pipette tip was applied to gently and slowly scratched across the center of the well. The cells were washed with 1× PBS and replaced with fresh serum-free medium. After wounding by Olympus IX73 microscope, the microscopic pictures were captured at 0 and 24h subsequently. Values were means ± standard deviation (SD) from at least three independent assays.

Statistical analysis

Statistical analyses were performed utilizing SPSS 17.0 statistical software package (SPSS Inc, Chicago, IL, USA). The association between ASF1B protein expression and histomorphological factors was accessed by Pearson’ chi-squared test and Fisher’s exact test. Spearman’s rank correlation coefficients were applied to evaluate the bivariate correlations between the variable factors. The overall survival (OS)

and the disease-free survival (DFS) in correlation with ASF1B protein expression were calculated using Kaplan-Meier analysis and compared using the log-rank test. Cox regression analyses(univariate and multivariate survival analyses) were performed to investigate survival data. *P* values less than 0.05 were considered statistically significant in all cases.

Results

Expression of ASF1B is elevated in human cervical cancer

Expression pattern of ASF1B mRNA and protein were examined in cervical cancer cell lines and tissues using qRT-PCR and analysis of western blotting. Compared with normal cervical samples, the ASF1B mRNA and protein were significantly overexpressed in cell lines of cervical cancer (Fig. 1, $P < 0.05$). Consistent with the results in cell lines, ASF1B transcriptional and translational expressions were significantly higher in the eight cervical neoplasm specimens than their expressions in the matched adjacent normal samples (Fig. 2, $P < 0.05$). Next, the ASF1B expression in 147 lesions was further investigated using IHC. Consistent with the above results, IHC showed elevated levels of the ASF1B protein expression in early-stage utertine cervical carcinoma specimens (Fig. 2C).

Overexpression of ASF1B protein correlates with the clinicopathologic characteristics of early-stage cervical carcinoma

To determine the relationship between ASF1B levels and clinical pathological parameters, and whether ASF1B could act as a new important prognostic biomarker, we determined the ASF1B levels in a cohort of 147 paraffin-embedded existing cervical neoplasm samples by IHC. The cervical carcinoma specimens for IHC included FIGO stage IB1 (61 cases, 41.5%), stage IB2 (24 cases, 16.3%), stage IIA1 (42 cases, 28.6%), and stage IIA2 (20 cases, 13.9%) disease. IHC analysis showed that ASF1B protein expression level was evaluated as negative or weakly positive in 61/147cases (41.5%), and positive in 86/147 (58.5%) cases. Positivity for ASF1B staining was mostly localized in the nucleus and rarely in epithelial cells cytoplasm (Fig. 3A). The mean response intensity of all positive cervical cancer cells in the field of vision was explored utilizing Mean optical density (MOD). The quantitative analysis demonstrated that the MOD of ASF1B protein were significantly increased in the subgroups with lymphovascular space involvement compared with that in the subgroups without lymphovascular space involvement (Fig. 3B, $P < 0.05$). The MOD values of ASF1B protein were lower in the subgroups without PLNM than in the subgroups with PLNM (Fig. 3C, $P < 0.05$). Furthermore, the correlation between the protein expression of ASF1B and pathological parameters was explored utilizing the Fisher's exact test and Chi-squared test. As summarized in Table 2, we didn't find any obvious association of ASF1B protein levels with age, histological type, tumor size, myometrium invasion, infiltration of the parauterine organ, tumor recurrence, or differentiation grade ($P > 0.05$). However, ASF1B protein overexpression was significantly associated with SCC-Ag ($P = 0.037$), FIGO stage ($P = 0.010$), property of surgical margin ($P = 0.036$), lymphovascular

space involvement($P < 0.001$), PLNM ($P = 0.022$), and even vital status ($P < 0.001$). The above relationships were further statistically analysed by Spearman's rank correlation test, which is summarized in Table 3.

Table 2
Correlation between ASF1B protein expression and the clinicopathological features of early-stage cervical cancer

Characteristic		Total	No or weak ASF1B expression	Moderate or strong ASF1B expression	Chi-squared test (*P*-value)	Fisher's exact test (*P*-value)
Age (years)	≤ 46	79	32 (21.8)	47 (32.0)	0.793	0.867
	> 46	68	29 (19.7)	39 (26.5)		
Histological type	Adenocarcinoma	9	3 (2.0)	6 (4.1)	0.608	0.736
	Squamous cell carcinoma	138	58 (39.5)	80 (54.4)		
FIGO stage	Ib1	61	34 (23.1)	27 (18.4)	0.010	-
	Ib2	24	8 (5.4)	16 (10.9)		
	IIa1	42	10 (6.8)	32 (21.8)		
	IIa2	20	9 (6.1)	11 (7.5)		
Pelvic lymph node metastasis	Absent	103	49 (34.0)	54 (36.7)	0.022	0.028
	Present	44	12 (8.2)	32 (21.8)		
Squamous cell carcinoma antigen, ng/ml	≤ 1.5	67	34 (23.1)	33 (22.4)	0.037	0.044
	> 1.5	80	27 (18.4)	53 (36.1)		
Tumor size, cm	< 4	107	48 (32.7)	59 (40.1)	0.176	0.193
	≥ 4	40	13 (8.8)	27 (18.4)		
Tumor recurrence	No	137	57 (38.8)	73 (49.7)	0.110	0.125
	Yes	10	4 (2.7)	13 (8.8)		
Vital status (at last follow-up)	Alive	115	59 (40.1)	56 (38.1)	< 0.001	< 0.001
	Dead	32	2 (1.4)	30 (20.4)		
Differentiation grade	G1	53	26 (17.7)	27 (18.4)	0.374	-
	G2	80	30 (20.4)	50 (34.0)		
	G3	14	5 (3.4)	9 (6.1)		
Chemotherapy	No	65	25 (17.0)	40 (27.2)	0.506	0.613
	Yes	82	36 (24.5)	46 (31.3)		
Radiation therapy	No	127	55 (37.4)	72 (49.0)	0.262	0.332

Characteristic		Total	No or weak ASF1B expression	Moderate or strong ASF1B expression	Chi-squared test (*P*-value)	Fisher's exact test (*P*-value)
	Yes	20	6 (4.1)	14 (9.5)		
Myometrium invasion	< 1/2	52	26 (17.7)	26 (17.7)	0.122	0.161
	≥ 1/2	95	35 (23.8)	60 (40.8)		
Property of surgical margin	No	137	60 (40.8)	77 (52.4)	0.036	0.046
	Yes	10	1 (0.7)	9 (6.1)		
Infiltration of parauterine organ	No	140	59 (40.1)	81 (55.1)	0.477	0.700
	Yes	7	2 (1.4)	5 (3.4)		
Lymphovascular space involvement	No	126	60 (40.8)	66 (44.9)	< 0.001	< 0.001
	Yes	21	1 (0.7)	20 (13.6)		

Table 3
Spearman correlation analysis of ASF1B protein expression versus clinicopathological features

Variable	ASF1B protein expression	
	Spearman's correlation coefficient	P-value
Age	0.022	0.795
Pelvic lymph node metastasis	0.189	0.022
Squamous cell carcinoma antigen, ng/ml	0.172	0.037
Tumor size	0.112	0.178
Recurrence	0.132	0.111
Histological type	0.042	0.611
Vital status	0.377	< 0.001
Chemotherapy	0.055	0.509
Radiation therapy	0.093	0.265
Myometrium invasion	0.128	0.123
Property of surgical margin	0.173	0.036
Infiltration of parauterine organ	0.059	0.480
Lymphovascular space involvement	0.304	< 0.001

Upregulation of ASF1B immunohistochemical expression is significantly correlated with unfavorable survival of patients with cervical carcinoma

To assess the association of ASF1B with survival in cervical neoplasm, we evaluated the relationship between the expression levels of ASF1B protein and clinical outcome in cohorts with early-stage cervical carcinoma. Notably, the survival curves showed that patients with ASF1B protein overexpression exhibited poorer OS and DFS compared with those with low expression of ASF1B protein in early-stage cervical cancer (log-rank, $P < 0.001$; Fig. 4A and 4B). In the low-ASF1B group, the cumulative rates of OS and DFS were 96.6% and 90.9% respectively while they were 57.7% and 78.0% respectively in the high-ASF1B group.

Additionally, the survival values of ASF1B protein expression pattern were calculated in different subgroups of cervical cancer cohorts, which were classified according to SCC-Ag, PLNM, age, tumor size, FIGO stage, properties of the surgical margin, differentiation grade, deep stromal invasion, lymphovascular space involvement, chemotherapy, radiotherapy, and parauterine organ infiltration. Interestingly, expression levels of ASF1B remarkably correlated with the duration of OS in patients with SCC-Ag (1.5 > ng/ml, log-rank test, $P = 0.012$; ≤ 1.5 ng/ml, log-rank test, $P < 0.001$), with or without PLNM (log-rank test, $P = 0.003$; log-rank test, $P = 0.001$), with age (> 46 years, log-rank test, $P < 0.001$, ≤ 46 years log-rank test, $P = 0.005$), with tumor size (tumor size ≥ 4 cm, log-rank test, $P = 0.014$; tumor size < 4 cm, log-rank test, $P < 0.001$), with FIGO stage (IB1–IB2, log-rank test, $P < 0.001$; IIA1–IIA2 log-rank test, $P = 0.002$), without property of the surgical margin (log-rank test, $P < 0.001$), with histological differentiation grade (Grade 1–2, log-rank test, $P < 0.001$; Grade 2–3, log-rank test, $P < 0.001$), without lymphovascular space involvement (log-rank test, $P < 0.001$), without infiltration of parauterine organ (log-rank test, $P < 0.001$), with or without myometrium invasion (log-rank test, $P < 0.001$; log-rank test, $P = 0.003$), and without radiotherapy (log-rank test, $P < 0.001$) (Fig. 5 and Fig. 6).

We subsequently detect whether ASF1B protein could serve as a novel prognostic factor using cox regression analysis. As detailed in Table 4, univariate analysis showed that ASF1B protein expression, PLNM, lymphovascular space involvement, and recurrence were strongly correlated with OS ($P < 0.05$). Multivariate Cox proportional hazards model analysis suggested that only ASF1B protein expression and tumor recurrence were independent risk predictors for the prognosis in cervical carcinoma ($P = 0.001$, 95% CI: 2.904–52.893; $P < 0.001$, 95% CI: 2.280–11.851; Table 4).

Table 4
Univariate and multivariate analyses of prognostic factors in early-stage cervical cancer using the Cox-regression model

	Univariate analysis			Multivariate analysis		
	No. of patients	*P*-value	Regression coefficient (SE)	*P*-value	Relative risk	95% CI
ASF1B		< 0.001	2.666 (0.732)	0.001	12.394	2.904–52.893
Low expression	67					
High expression	80					
Pelvic lymph node metastasis		0.007	0.953 (0.354)	0.153	1.706	0.820–3.550
Absent	103					
Present	44					
Lymphovascular space involvement		0.020	0.915 (0.393)	0.376	0.668	0.274–1.632
No	126					
Yes	21					
Recurrence		< 0.001	1.862 (0.379)	< 0.001	5.198	2.280–11.851
No	137					
Yes	10					

Silencing of ASF1B attenuates migration and invasion in CasKi and Siha cells

Our result found that ASF1B protein is significantly correlated to lymph node metastasis. As we know, cell migration and invasion are strongly associated with tumor metastasis. Thus, we analysed gene expression array data publicly available online, which was used in Gene Set Enrichment Analysis (GSEA) for ASF1B. The result showed that upregulation of ASF1B was correlated with tumor metastasis (Fig. 7A). Next, we carried out a transwell migration assay and a wound healing assay. In transwell assay, the results showed that silencing ASF1B obviously reduced the number of cells on membrane filters (Fig. 7B). Consistently, the results of wound healing assays found that the effect of ASF1B inhibition on the invasiveness of CasKi and Siha cells was remarkably hampered (Fig. 7C). Overall, these results suggested that inhibition of ASF1B weakened the invasion and migration properties of cervical cancer cells.

Silencing of ASF1B inhibited the Wnt/β-catenin signaling pathway in cerivcal carcinoma

We used GSEA to further detect the potential mechanism by which ASF1B promotes the invasion and migration capacities of cervical carcinoma cells. The result demonstrated that upregulation of ASF1B was correlated with Wnt/β-catenin signaling pathway (Fig. 8A). Since Wnt/β-catenin signalling pathway is regarded as a key regulator of CSC self-renewal, we hypothesized that ASF1B may activate Wnt/β-catenin signalling pathway and therefore promote stem cell-like capacities and tumourigenic potential in cervical neoplasm. We detected the effect of ASF1B on the subcellular localization of β-catenin to validate this hypothesis. Interestingly, repression of ASF1B expression hampered, the translocation of β-catenin into the nucleus, as demonstrated by Western blotting results of nuclear and cytoplasmic cellular components (Fig. 8C). Next, we identified that the expression pattern of Wnt/β-catenin signaling pathway-related genes, including c-Myc and cyclin D1. The results found that the expression levels of c-Myc and cyclin D1 proteins were strongly decreased in ASF1B silencing cells (Fig. 8B). All the data mentioned above indicated that ASF1B may regulate the Wnt/β-catenin signaling pathway in cervical carcinoma.

Discussion

The current study showed that compared with that in matched adjacent non-cancerous cervical specimens, the ASF1B expression was remarkably overexpressed in human cervical carcinoma lesions at both the transcription and translation levels. High ASF1B protein levels were associated with clinical characteristics such as FIGO stage, SCC-Ag, PLNM, lymphovascular space involvement, property of surgical margin, and even vital status. The results showed that measurement of the ASF1B protein level is a promising independent tool to test or predict survival of the sufferers with early-stage cervical carcinoma. Furthermore, in vitro assays indicated that inhibition of ASF1B expression hampered the invasiveness and migration of cervical cancer cells through regulating Wnt/β-catenin signaling pathway. Our results revealed a mechanism that enhances tumor metastasis in cervical neoplasm, which implied that ASF1B had potential to be an important therapeutic target for cervical carcinoma treatment.

In previous studies, ASF1B was proven to have an important role in tumors, which is consistent with findings from our study. ASF1B exists as a distinct isoform of ASF1 in humans. ASF1, originally found in budding yeast because of its effect on heterochromatin silencing, is the most conserved histone H3/H4 chaperone protein from yeast to humans. The most important ASF1-dependent acetylation target sites in mammals are H3K56 and H3K56 acetylation, which are culpably involved in genome stability, DNA replication, stem cell pluripotency, and cancers [13–16]. Seol et al. [17] found that H3K56 acetylation increased with increasing levels of ASF1B in Hela cells, which makes ASF1B an fascinating therapeutic target for cancer treatment. It has been demonstrated that ASF1B served as a novel survival-related biomarker that correlates with poor tumor grade with relevance to the clinical outcome in breast cancer [11–12]. Moreover, ASF1B is an important prognostic factor for tumor metastasis and exerts a critical role in cell proliferation. ASF1B was highlighted in the prominent biology, which was related to the response of

colon carcinoma cells to bortezomib. ASF1B played an important role in proteasome depression–induced cell apoptosis, exactly polyamine dysregulation, mTOR ablation, and DNA damage signaling enhancement [18]. Co-exhaustion of the histone chaperones ASF1A and ASF1B yielded all typical biomarks of alternative lengthening of telomeres (ALT) in both primary and tumor cells, which is positively regulated by RAD17 checkpoint clamp loader component (RAD17) and Bloom syndrome RecQ like helicase (BLM), and negatively regulated by exonuclease 1 (EXO1) and DNA Replication Helicase/Nuclease 2 (DNA2) [19]. In addition, ASF1B is targeted by microRNA miR-214 in myeloma. These studies indicated that ASF1B may be directly or indirectly involved in the progression of various tumors through different molecular mechanisms. In our cohort, ASF1B was found up-regulated at both the transcriptional and translational levels in cervical carcinoma. We showed the relationship between ASF1B expression and some clinical high risk factors, which indicated that ASF1B is an important predictor that correlates with tumor development and progression in cervical carcinoma. Collectively, our results suggested that ASF1B overexpression is a new independent indicator for poor survival in human malignancies. Wnt/β-catenin signaling pathway exerts a regulatory role in a series of cellular events, including cell invasion, proliferation and differentiation via regulating the capacity of the multifunctional β-catenin protein[20]. It is reported that Wnt/β-catenin signaling is often aberrantly activated during the carcinogenesis and aggressiveness of cervical malignancy[21]. Wnt pathway was previously reported to exert a great impact on regulation of cell migration and appears to be an important step during cervical carcinogenesis[22]. Nevertheless, little is known about the correlation between ASF1B and Wnt/β-catenin signaling in cervical cancer metastasis. Our results indicated that inhibition of ASF1B may repress invasion and migration via Wnt/β-catenin signaling in uterine cervical neoplasm. These data mentioned above have provided new insights into the tumor development and progression of cervical cancer. However, the precise mechanisms that link ASF1B to the metastatic process in cervical cancer are unclear and require further research.

Treatment strategies are strongly correlated with prognosis in cervical cancer patients. Various treatment strategies cause different types and degrees of side effects in patients. Clinically, the current standard treatment for early-stage cervical carcinoma remains radical hysterectomy, plus lymphadenectomy (RH) or concurrent chemoradiotherapy (CCRT). According to the guidelines for the treatment of cervical carcinoma, such as those of the National Comprehensive Cancer Network [23], National Cancer Institute [24], and the European Society of Medical Oncology [25], patients with intermediate or high risk factors should receive radiation therapy (RT) or CCRT as the standard supplementary therapy after RH. Positive lymphovascular space involvement is one of the intermediate or advanced-disease indicators of cervical carcinoma. Patients diagnosed with positive lymphovascular space involvement will receive postoperative chemotherapy and/or RT. Recent studies indicated that CCRT and RT are equally effective for patients with early-stage cervical neoplasm [26]. Patients who receive CCRT instead of unnecessary surgical treatment can avoid surgery-related side effects, including intra- and postoperative bleeding, inflammation, deep vein thrombosis, pelvic lymphocytes, lymphedema (tissue swelling), and elephantiasis (tissue/skin thickening). Furthermore, lymphovascular space involvement is an independent risk factor that is remarkably associated with poor clinical outcome in cervical carcinoma

[27]. Thus, it is important to identify patients with positive lymphovascular space involvement. Deng et al. [28] found that Stomatin-like protein 2 (SLP-2) may be a progressive gene in the development of cervical cancer and correlates with lymphovascular space involvement. It is reported that WNT2 overexpression was correlated with lymphovascular space involvement in cervical cancer [29]. Moreover, overexpression of the kinesin family member 20A (KIF20A) protein was demonstrated to be strongly associated with lymphovascular space involvement in carcinoma of the uterine cervix [30]. However, currently, few suitable tumor markers can be applied to predict lymphovascular space involvement in the clinical setting. Here, our data revealed that upregulation of ASF1B is significantly associated with positive lymphovascular space involvement in cervical cancer. Additionally, a relationship between OS and ASF1B protein overexpression was detected in the “without lymphovascular space involvement” and “with lymphovascular space involvement” subgroups. Finally, a significant correlation between poorer OS and ASF1B upregulation was observed in the subgroup of “without lymphovascular space involvement”, which indicated that ASF1B might serve as a potential marker for clinical outcome prediction of patients with cervical cancer without lymphovascular space involvement. Nevertheless, Cox regression analysis determined that lymphovascular space involvement is not an independent prognostic biomarker of cervical cancer. One explanation may be that there were insufficient cases of lymphovascular space involvement among the recruited patients. Thus, relevant research extended to a larger cohort of patients diagnosed with lymphovascular space involvement is needed. More studies should be planned and performed to explore the related molecular mechanisms of the relationship between ASF1B expression and lymphovascular space involvement in cervical carcinoma.

Pelvic lymph node metastasis (PLNM) exerts a pitoval and direct role in prediction of the survival of cervical cancer patients, additionally determining the optimal therapeutic arrangements [31]. For patients with PLNM, CCRT is needed, which in retrospect, would cause the initial surgical procedure unnecessary. Currently, no precise molecular marker has been found to identify patients with PLNM to avoid improper treatment and access to better clinical decision making. Thus, there is an urgent need to identify an ideal preoperative marker to predict PLNM in cervical carcinoma. The current study showed that aberrant ASF1B protein expression was largely correlated with PLNM in cervical carcinoma. In univariate analysis, the result suggested that PLNM might be a prognostic predictor in patients with early-stage cervical carcinoma, which is similar to previous studies [32–33]. Notably, ASF1B protein overexpression was remarkably associated with worse postoperative OS of patients with cervical carcinoma in subgroups with or without PLNM. This indicated that different levels of ASF1B protein expression can help clinics to identify patients with poorer clinical outcome, which will lead to more aggressive treatment for these sufferers to decrease the tumor-related deaths. Nevertheless, no significant correlation was determined between ASF1B protein expression and PLNM in cervical cancer. In future work, extensive researches with a larger-scale sample are necessary to understand the role and detailed mechanisms of ASF1B protein expression’s effects on PLNM in cervical carcinoma.

In conclusion, this study indicated that ASF1B is overexpressed in cervical carcinoma and elevated ASF1B expression is an independent prognostic predictor which significantly associated with SCC-Ag, FIGO stage, property of surgical margin, lymphovascular space involvement and PLNM. Moreover, we

domonstrated that ASF1B modulated the cell invasion and migration of cervical cancer cell lines via the Wnt/β-catenin pathway. Our findings supplied some new views in studies of the development of cervical cancer, which may lead to novel tumor therapies.

Declarations

Acknowledgements

This work was supported by grants from the National Natural Science Foundation of China (No.81902638 and 81872124).

Declaration of Conflict of Interest

None.

References

[1] Wenzel L, Dogan-Ates A, Habbal R, Berkowitz R, Goldstein DP, et al. Defining and measuring reproductive concerns of female cancer survivors. J Natl Cancer Inst Monogr. 2005; 94–98.

[2] Ferlay J, Soerjomataram I, Ervik M, Dikshit R, Eser S, Mathers C, et al. GLOBOCAN 2012 v1.0, Cancer Incidence and Mortality Worldwide: IARC CancerBase No. 11 [Internet]. International Agency for Research on Cancer: Lyon, France; 2013. Available from: http://globocan.iarc.fr. Accessed on 26 Mar 2015.

[3] Zhang W, He W, Shi Y, Gu H, Li M, Liu Z, et al. High Expression of KIF20A Is Associated with Poor Overall Survival and Tumor Progression in Early-Stage Cervical Squamous Cell Carcinoma. PLoS One. 2016 Dec 12;11(12):e0167449.

[4] Liu L, Xia M, Wang J, Zhang W, Zhang Y, He M. CISD2 expression is a novel marker correlating with pelvic lymph node metastasis and prognosis in patients with early-stage cervical cancer. Med Oncol. 2014 Sep;31(9):183.

[5] Wang XJ, Xiong Y, Ma ZB, Xia JC, Li YF. The expression and prognostic value of protein tyrosine kinase 6 in early-stage cervical squamous cell cancer. Chin J Cancer. 2016 Jun 16;35(1):54.

[6] Zhang W, Hou T, Niu C, Song L, Zhang Y. B3GNT3 Expression Is a Novel Marker Correlated with Pelvic Lymph Node Metastasis and Poor Clinical Outcome in Early-Stage Cervical Cancer. PLoS One. 2015 Dec 28;10(12):e0144360.

[7] Zhang W, He W, Shi Y, Zhao J, Liu S, Zhang F, Yang J, Xie C, Zhang Y. Aberrant TIMELESS expression is associated with poor clinical survival and lymph node metastasis in early-stage cervical carcinoma. Int J Oncol. 2017 Jan;50(1):173-184.

[8] Mello JA, Sillje HH, Roche DM, Kirschner DB, Nigg EA, Almouzni G. Human Asf1 and CAF-1 interact and synergize in a repair-coupled nucleosome assembly pathway. EMBO Rep 2002,3(4):329-334

[9] Messiaen S, Guiard J, Aigueperse C, Fliniaux I, Tourpin S, Barroca V, Allemand I, Fouchet P, Livera G, Vernet M. Loss of the histone chaperone ASF1B reduces female reproductive capacity in mice. Reproduction. 2016 May;151(5):477-89.

[10] Paul PK, Rabaglia ME, Wang CY, Stapleton DS, Leng N, Kendziorski C, Lewis PW, Keller MP, Attie AD. Histone chaperone ASF1B promotes human β-cell proliferation via recruitment of histone H3.3. Cell Cycle. 2016 Dec;15(23):3191-3202.

[11] Corpet A, De Koning L, Toedling J, Savignoni A, Berger F, Lemaître C, O'Sullivan RJ, Karlseder J, Barillot E, Asselain B, Sastre-Garau X, Almouzni G. Asf1b, the necessary Asf1 isoform for proliferation, is predictive of outcome in breast cancer. EMBO J. 2011 Feb 2;30(3):480-93.

[12] Montes de Oca R, Gurard-Levin ZA, Berger F, Rehman H, Martel E, Corpet A, de Koning L, Vassias I, Wilson LO, Meseure D, Reyal F, Savignoni A, Asselain B, Sastre-Garau X, Almouzni G. The histone chaperone HJURP is a new independent prognostic marker for luminal A breast carcinoma. Mol Oncol. 2015 Mar;9(3):657-74.

[13] Das C, Lucia MS, Hansen KC and Tyler JK (2009) CBP/p300-mediated acetylation of histone H3 on lysine 56. Nature 459, 113-117

[14] Han J, Zhou H, Horazdovsky B, Zhang K, Xu RM and Zhang Z (2007) Rtt109 acetylates histone H3 lysine 56 and functions in DNA replication. Science 315, 653-655

[15] Tan Y, Xue Y, Song C and Grunstein M (2013) Acetylated histone H3K56 interacts with Oct4 to promote mouse embryonic stem cell pluripotency. Proc Natl Acad Sci, USA 110, 11493-11498

[16] Battu A, Ray A and Wani AA (2011) ASF1A and ATM regulate H3K56-mediated cell-cycle checkpoint recovery in response to UV irradiation. Nucleic Acids Res 39, 7931-7945

[17] Seol JH, Song TY, Oh SE, Jo C, Choi A, Kim B, Park J, Hong S, Song I, Jung KY, Yang JH, Park H, Ahn JH, Han JW, Cho EJ.Identification of small molecules that inhibit the histone chaperone Asf1 and its chromatin function. BMB Rep. 2015 Dec;48(12):685-90.

[18] Bexiga MG, Simpson JC. Genome-Wide siRNA Screen for Modulators of Cell Death Induced by Proteasome Inhibitor Bortezomib.Methods Mol Biol. 2016;1470:39-48.

[19] O'Sullivan RJ, Arnoult N, Lackner DH, Oganesian L, Haggblom C, Corpet A, Almouzni G, Karlseder J. Rapid induction of Alternative Lengthening of Telomeres by depletion of the histone chaperone ASF1. Nat Struct Mol Biol. 2014 Feb;21(2):167-174.

[20] H. Clevers, R. Nusse, Wnt/b-catenin signaling and disease, Cell 149 (6) (2012) 1192–1205.

[21] A. Üren, S. Fallen, H. Yuan, et al., Activation of the canonical Wnt pathway during genital keratinocyte transformation: a model for cervical cancer progression, Cancer Res. 65 (14) (2005) 6199–6206.

[22] Yang M, Wang M, Li X, Xie Y, Xia X, Tian J, Zhang K, Tang A. Wnt signaling in cervical cancer? J Cancer. 2018 Mar 20;9(7):1277-1286.

[23] NCCN Clinical Guideline in Oncology. Cervical Cancer Version 2, 2015. Available online: http://www.nccn.org/professionals/physician_gls/pdf/cervical.pdf (accessed on 23 August 2015).

[24] Cervical Cancer Treatment (PDQ). Available online: http://www.cancer.gov/cancertopics/pdq/treatment/ cervical/Patient/page5 (accessed on 22 October 2014).

[25] Colombo, N.; Carinelli, S.; Colombo, A.; Marini, C.; Rollo, D.; Sessa, C. Cervical cancer: ESMO clinical practice guidelines for diagnosis, treatment and follow-up. Ann. Oncol. 2012, 23, vii27–vii32.

[26] Niu C, Sun X, Zhang W, Li H, Xu L, Li J, Xu B, Zhang Y. NR2F6 Expression Correlates with Pelvic Lymph Node Metastasis and Poor Prognosis in Early-Stage Cervical Cancer. Int J Mol Sci. 2016 Oct 20;17(10).

[27] Shen HW, Tan JF, Shang JH, Hou MZ, Liu J, He L, Yao SZ, He SY. CPE overexpression is correlated with pelvic lymph node metastasis and poor prognosis in patients with early-stage cervical cancer. Arch Gynecol Obstet. 2016 Aug;294(2):333-342.

[28] Deng H, Deng Y, Liu F, Chen J, Li Z, Zhao K, Guan X, Liang W. Stomatin-like protein 2 is overexpressed in cervical cancer and involved in tumor cell apoptosis. Oncol Lett. 2017 Dec;14(6):6355-6364.

[29] Zhou Y, Huang Y, Cao X, Xu J, Zhang L, Wang J, Huang L, Huang S, Yuan L, Jia W, Yu X, Luo R, Zheng M. WNT2 Promotes Cervical Carcinoma Metastasis and Induction of Epithelial-Mesenchymal Transition. PLoS One. 2016 Aug 11;11(8):e0160414.

[30] Zhang W, He W, Shi Y, Gu H, Li M, Liu Z, Feng Y, Zheng N, Xie C, Zhang Y. High Expression of KIF20A Is Associated with Poor Overall Survival and Tumor Progression in Early-Stage Cervical Squamous Cell Carcinoma. PLoS One. 2016 Dec 12;11(12):e0167449.

[31] Yang S, Liu Y, Xia B, Deng J, Liu T, Li Q, Yang Y, Wang Y, Ning X, Zhang Y, Xiao M. DLL4 as a predictor of pelvic lymph node metastasis and a novel prognostic biomarker in patients with early-stage cervical cancer. Tumour Biol. 2016 Apr;37(4):5063-74.

[32] Selman TJ, Mann C, Zamora J, Appleyard TL, Khan K. Diagnostic accuracy of tests for lymph node status in primary cervical cancer: a systematic review and meta-analysis. CMAJ. 2008;178(7):855–862.

[33] Li Z, Yu CP, Zhong Y, Liu TJ, Huang QD, Zhao XH, et al. Sam68 expression and cytoplasmic localization is correlated with lymph node metastasis as well as prognosis in patients with early-stage

cervical cancer. Ann Oncol. 2012 Mar; 23(3):638–646.

Figures

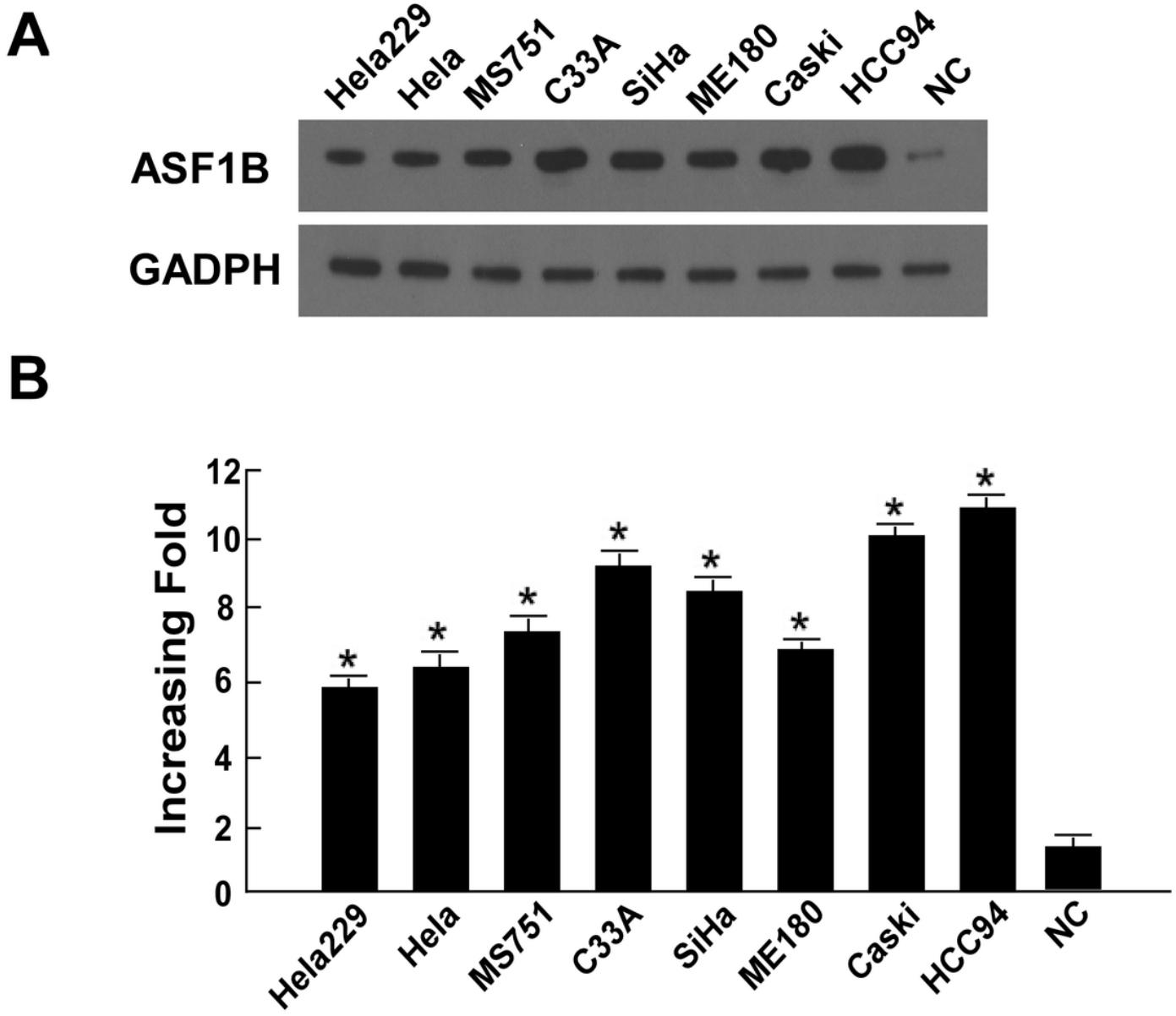

Figure 1

ASF1B mRNA and protein were overexpressed in cervical cancer cell lines. A, B The expression of ASF1B mRNA and protein in cervical cancer cell lines (HeLa229, HeLa, MS751, C33A, SiHa, ME180, CasKi, HCC94) and normal cervical tissue were examined by western blotting (A) and real-time PCR (B). Expression levels were normalized to the expression of GAPDH. Error bars represent the standard deviation of the mean (SD) calculated from three parallel experiments. *P < 0.05.

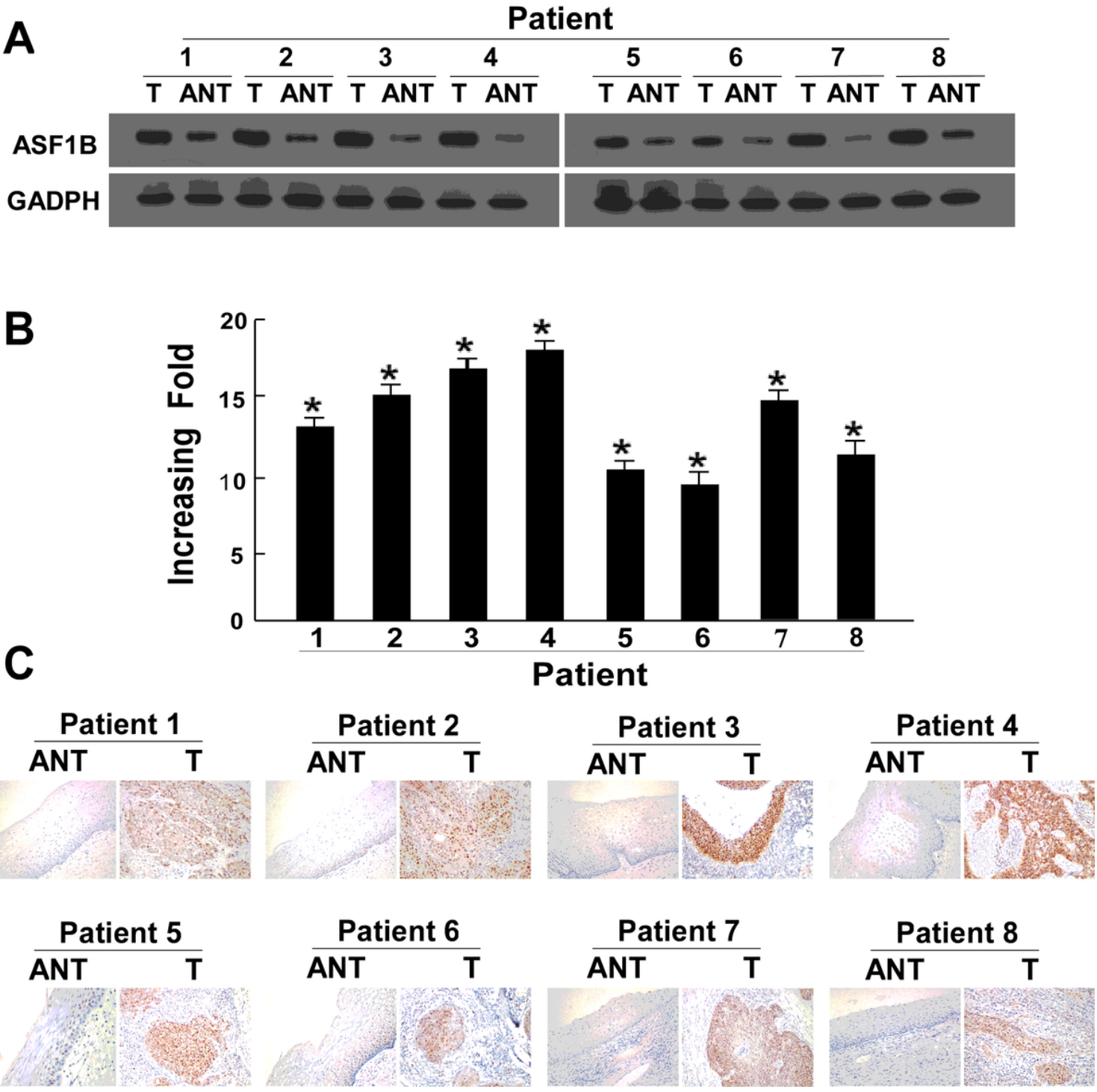

Figure 2

Upregulation of ASF1B mRNA and protein in early-stage cervical cancer specimens. (A) Representative pictures of western blotting analyses of ASF1B protein expression in eight matched pairs of cervical cancer tissue samples (T) and adjacent noncancerous tissues (ANT). GADPH was used as the loading control. (B) The average T/ANT ratios of ASF1B mRNA expression in the paired cervical cancer (T) and adjacent noncancerous tissue sections (ANT) were quantified using real-time PCR and normalized against the expression of GAPDH. The error bars represent the standard deviation of the mean (SD),

which was calculated from three parallel experiments. (C) Immunohistochemical detection of the ASF1B protein in eight pairs of matched early-stage cervical cancer tissues. *P < 0.05.

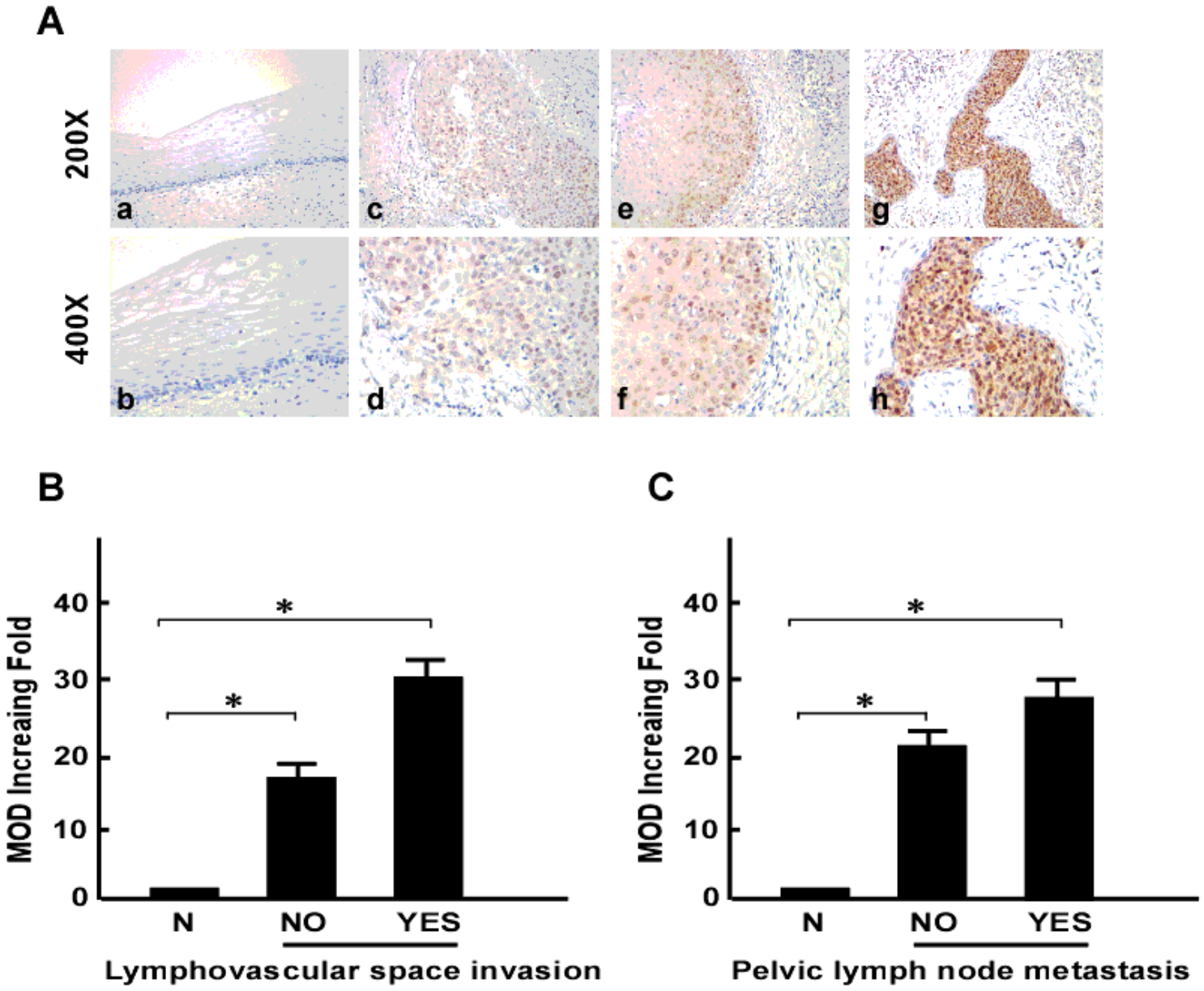

Figure 3

The expression of the ASF1B protein in paraffin-embedded tissues. ASF1B staining was mainly observed in the nucleus and rarely in the cytoplasm of cervical cancer cells. (A) a and b, ASF1B protein expression was not detected in normal cervical tissues; c and d, representative images of weak ASF1B staining in cervical cancer tissues; e and f, representative images of moderate ASF1B staining in cervical cancer tissues; g and h, representative images of strong ASF1B staining in cervical cancer tissues. (B) The statistical analyses of the average mean optical density (MOD) of ASF1B staining in the lymphovascular space involvement group and the lymphovascular space involvement-free group. (C) The statistical analyses of the average mean optical density (MOD) of ASF1B staining in the PLNM group and the PLNM-free group. *P < 0.05.

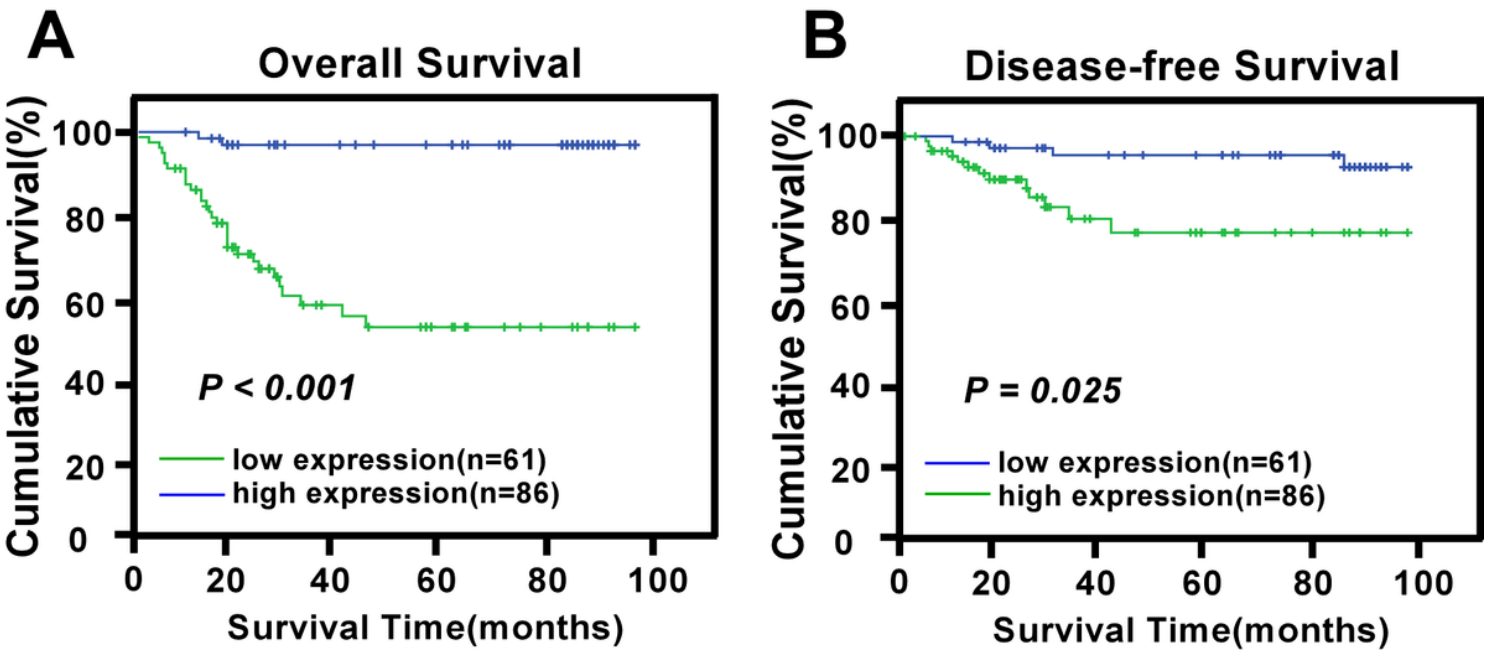

Figure 4

Kaplan–Meier curves for the univariate analysis data (log-rank test). The overall survival (A, OS) and disease-free survival (B, DFS) for patients with high versus low ASF1B protein expression.

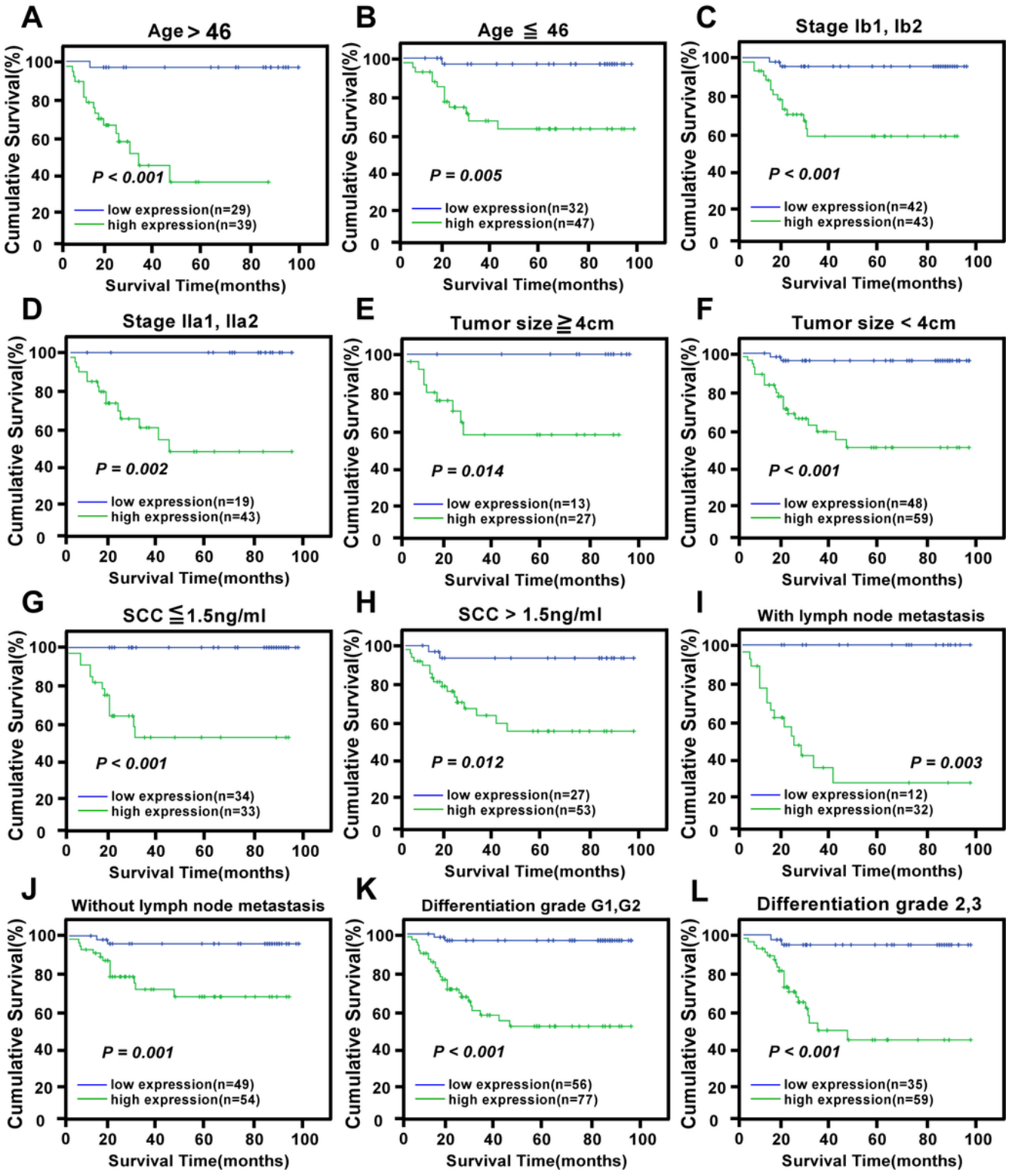

Figure 5

Survival curves for patients in selected subgroups (log-rank test). Survival curves for the patients (A) with age > 46 years; (B) with age ≤ 46 years; (C) at stages Ib1-Ib2; (D) at stages IIA1-IIA2; (E) with tumor size ≥ 4cm, (F) with tumor size < 4cm; (G) with SCC ≤ 1.5 ng/ml; (H) with SCC > 1.5 ng/ml; (I) with lymph node metastasis; (J) without lymph node metastasis; (K) at differentiation grade 1–2; and (L) at differentiation grade 2–3. (P < 0.05, respectively).

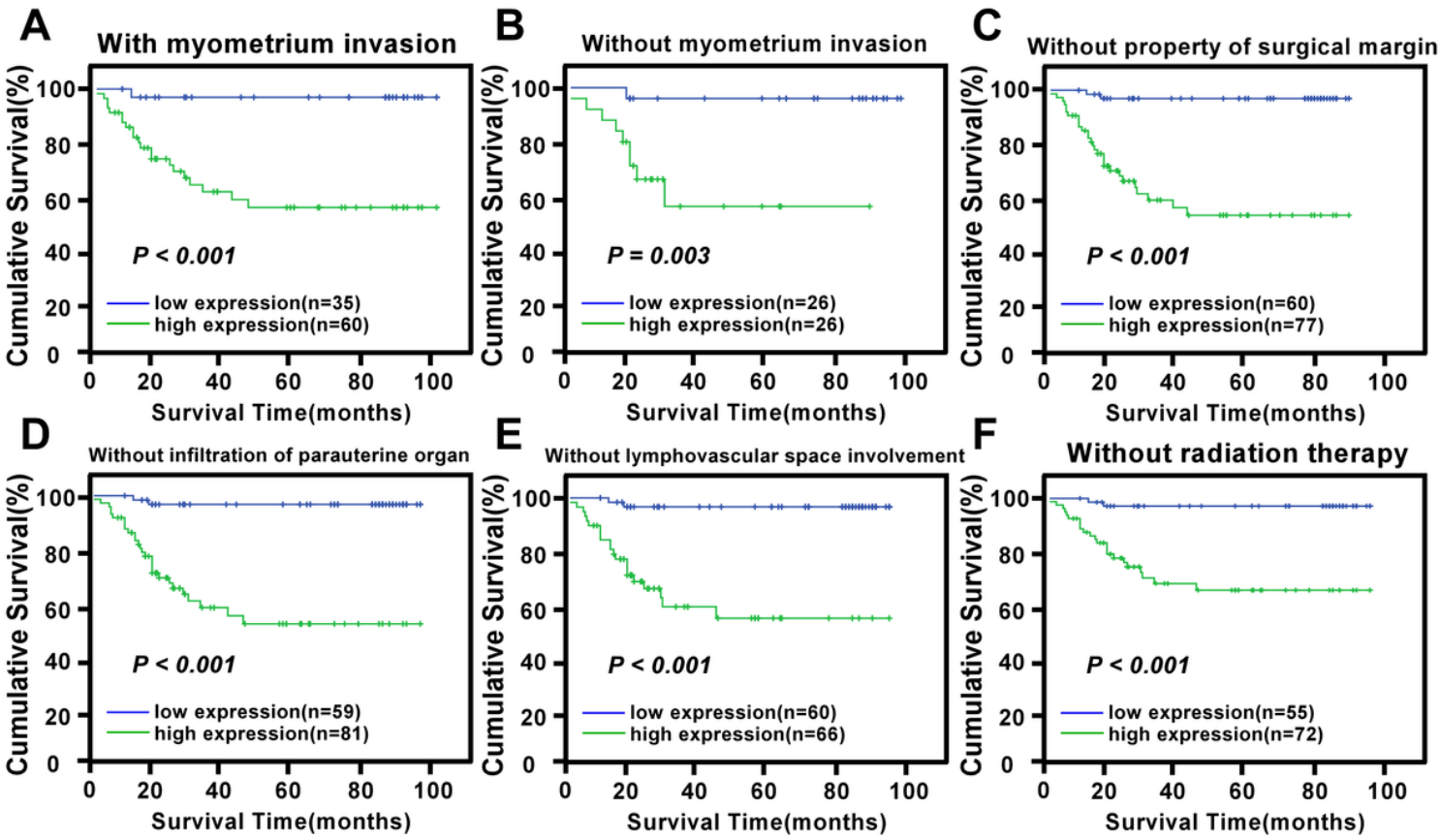

Figure 6

Survival curves for patients in selected subgroups (log-rank test). Survival curves for patients (A) with myometrium invasion; (B) without myometrium invasion; (C) without property of surgical margin; (D) without infiltration of parauterine organ; (E) without lymphovascular space involvement; and (F) without radiation therapy. ($P < 0.05$, respectively).

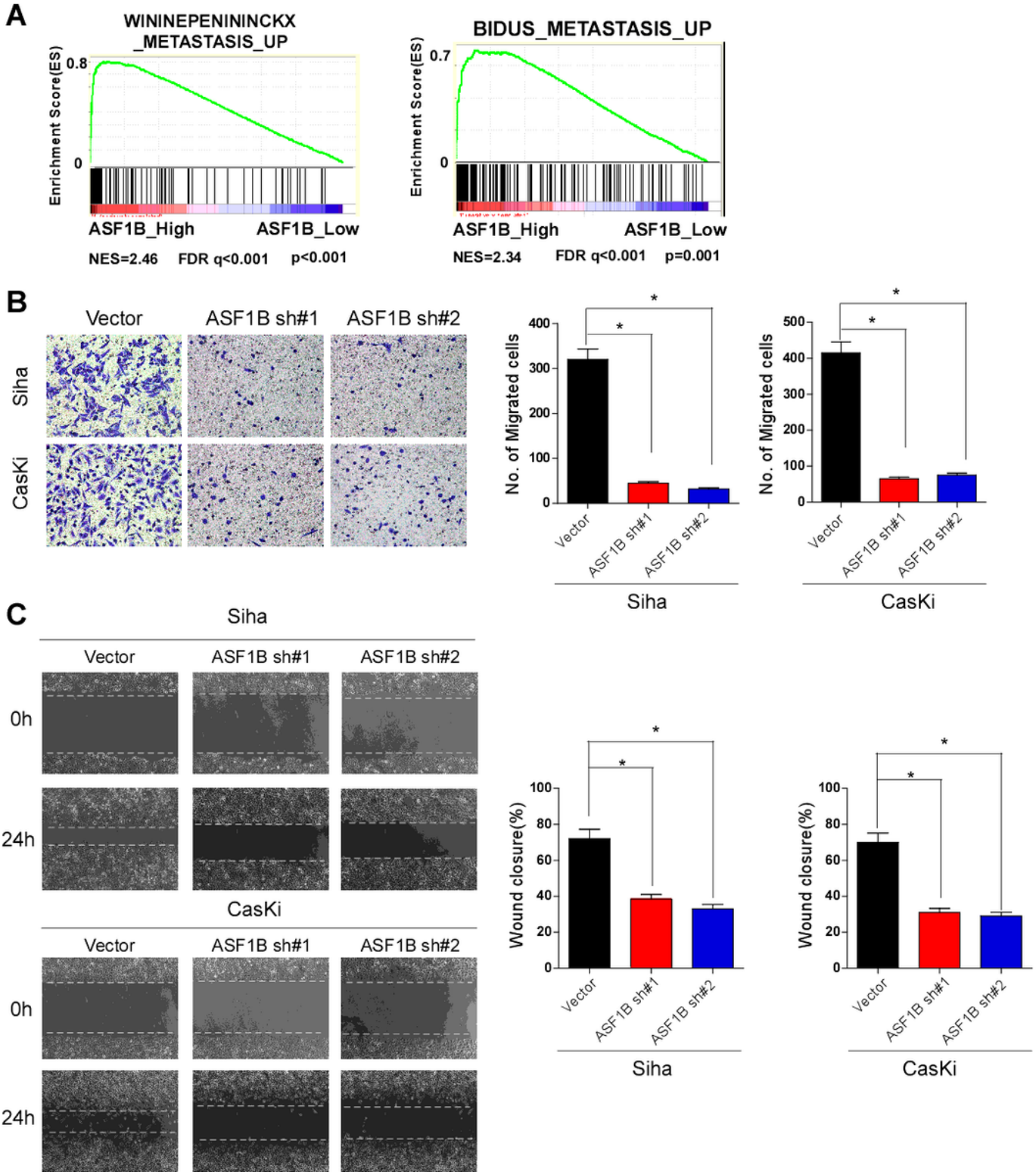

Figure 7

Downregulation of ASF1B inhibits the migration and invasion capacities of cervical cancer cell in vitro. (A) GSEA plots showed that ASF1B expression positively associated with tumor metastasis. (B) Transwell cell invasion assay of Siha and CasKi cells were carried out to detect invasive properties. (C) Wound healing assay was applied to evaluate the Mobility of tumor cells at 0 and 24 h (×200). Quantification of migration distance of Siha and CasKi cells cells (*P<0.05).

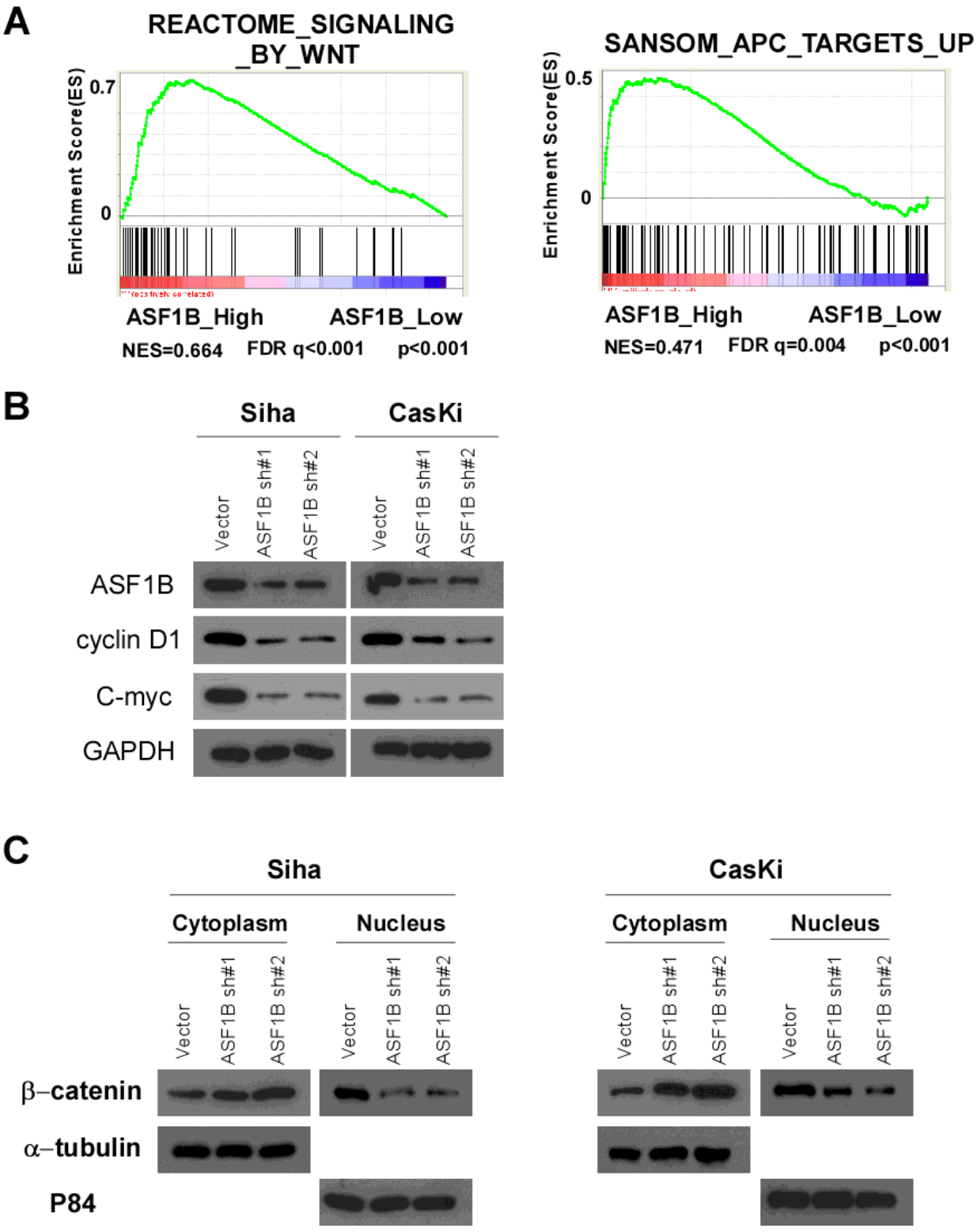

Figure 8

Silencing of ASF1B inactivated Wnt/β-catenin signaling pathway. (A) GSEA plots indicated that ASF1B expression positively associated with Wnt/β-catenin pathway in published cervical cancer gene expression profiles. (B) Western blotting analysis showed a significant relationship between ASF1B expression and the expression of cyclin D1 and c-Myc, the key downstream effectors of Wnt/β-catenin pathway. (*P<0.05). (C) Western blotting results of β-catenin protein levels in the nucleus and cytoplasm

of the Siha and CasKi cells. p84 and α-Tubulin were utilized as loading controls for the nuclear and cytoplasmic fractions, respectively.